

Efficient safe learning for controller tuning with experimental validation

Marta Zagorowska^a, Christopher König^b, Hanlin Yu^c, Efe C. Balta^b, Alisa Rupenyan^d, John Lygeros^c

^a*Department of Engineering Cybernetics, Norwegian University of Science and Technology, Trondheim, Norway, marta.zagorowska@ntnu.no (corresponding author)*

^b*Control and Automation Group, Inspire AG, Switzerland, efe.balta@inspire.ch*

^c*Automatic Control Laboratory, ETH Zürich, Switzerland, hanlyu@student.ethz.ch, lygeros@ethz.ch*

^d*ZHAW Centre for Artificial Intelligence, ZHAW Zürich University of Applied Sciences, Switzerland, rupn@zhaw.ch*

Abstract

Optimization-based controller tuning is challenging because it requires formulating optimization problems explicitly as functions of controller parameters. Safe learning algorithms overcome the challenge by creating surrogate models from measured data. To ensure safety, such data-driven algorithms often rely on exhaustive grid search, which is computationally inefficient. In this paper, we propose a novel approach to safe learning by formulating a series of optimization problems instead of a grid search. We also develop a method for initializing the optimization problems to guarantee feasibility while using numerical solvers. The performance of the new method is first validated in a simulated precision motion system, demonstrating improved computational efficiency, and illustrating the role of exploiting numerical solvers to reach the desired precision. Experimental validation on an industrial-grade precision motion system confirms that the proposed algorithm achieves 30% better tracking at sub-micrometer precision as a state-of-the-art safe learning algorithm, improves the default auto-tuning solution, and reduces the computational cost seven times compared to learning algorithms based on exhaustive search.

Keywords: Active learning, Controller tuning, Bayesian optimization, Safe learning, Gaussian process regression

1. Introduction

Optimizing controller parameters while ensuring safety is an important task in manufacturing, especially in systems where sub-micrometer precision is required. Solving such optimization problems can be challenging because of the unavailability of explicit formulations with respect to controller parameters and the computational cost of finding a solution (Skogestad, 2023). This paper builds on Bayesian optimization to find a constrained optimum of an unknown but measurable function in an efficient way.

The idea of using surrogate models for safety has been used in reliability engineering (Xu and Saleh, 2021). Several algorithms using Gaussian processes to approximate unknown safety constraints have been proposed, among others by Bichon et al. (2011), Fauriat and Gayton (2014), and Aziz-soltani and Sadeghi (2018). The main focus of these algorithms was to explore the search space safely, without explicitly finding the optimum. The SafeOpt algorithm proposed by Sui et al. (2015a) and extended by Berkenkamp et al. (2016) is an iterative algorithm that uses Gaussian processes to learn the unknown functional form of both the objective and the constraints. It builds on the Bayesian optimization algorithm proposed by Srinivas et al. (2012), where the upper bound of the Gaussian process corresponding to the objective function was considered to find the next iterate, without explicitly considering its safety. SafeOpt ensures the safety of chosen points in every iteration based on confidence intervals from the Gaussian processes. The choice of the new points is made by analyzing the safety of selected points from the whole search space, which requires evaluation over possibly large parameter sets (Aziz-soltani and Sadeghi, 2018). Since looking at the whole search space is equivalent to performing an exhaustive search, existing methods can quickly become computationally expensive, as indicated by Fiducioso et al. (2019) and Berkenkamp et al. (2021).

The version of SafeOpt from Sui et al. (2015b) requires knowledge about Lipschitz constants of the underlying functions, which limited the use of SafeOpt in practical settings. A modification proposed by Berkenkamp et al. (2016) removed the need for knowing the Lipschitz constants and has been successfully used for controller tuning, as shown by Khosravi et al. (2022). A review of approaches to using Bayesian optimization to controller tuning was done by Mesbah et al. (2022). Experimental performance of Bayesian optimization in controller tuning was shown by Fujimoto et al. (2022) where the authors initialized Gaussian processes with a simplified model of a plant.

These simplifications improve the computational cost by modifying how the next iterate is found in SafeOpt. However, these simplifications still rely on a discretization of the search space, which limits their practical usage.

A review of methods related to SafeOpt is given in Kim et al. (2021), where most of the reported algorithms use a discretized search space to find the optimum. The idea of merging optimization with safe learning was explored by Duivenvoorden et al. (2017), where the recommended point is computed by solving auxiliary optimization problems with particle swarm methods. The method preserves the idea of SafeOpt to use confidence intervals of Gaussian processes in every iteration but redefined the way of choosing new points to make it suitable for particle swarm methods. Due to the heuristic nature of particle swarm methods, the approach needs adjustments to ensure good performance of the swarm.

A grid-free version of SafeOpt using the solutions of local optimization problems to improve run time has been recently proposed by Zagorowska et al. (2023). The exhaustive search has been reformulated as a series of optimization problems to find the next recommended point. The reformulation allows avoiding heuristics while preserving the way the new points are chosen in every iteration of SafeOpt and improving the computational performance of the algorithm. The grid-free method has been shown to work in simulation (Zagorowska et al., 2023). However, the influence of solving local optimization problems instead of global grid search has not yet been analyzed in detail or demonstrated in real-world experiments.

In this work, we extend the grid-free SafeOpt from Zagorowska et al. (2023) to include a systematic way of initializing the local optimization problems. The contributions of the paper are:

- We reformulate SafeOpt as a series of optimization problems preserving the way new points are chosen in every iteration;
- We propose an initialization method for the reformulated algorithm ensuring feasibility in every iteration;
- We demonstrate the performance of the reformulated algorithm in a real precision motion system.

The results are compared with a benchmark algorithm for controller tuning for precision motion systems developed by König et al. (2021), and with the industrial autotuner provided by the equipment manufacturer.

The paper is structured as follows. We first provide the necessary background knowledge on Gaussian processes and SafeOpt in Section 2. Section 3 introduces the grid-free reformulation of SafeOpt while Section 4 discusses the necessary steps for using numerical solvers in grid-free SafeOpt. Section 5 presents the performance of the new algorithm in a simulation framework, whereas Section 6 presents the results of applying grid-free and grid SafeOpt in an experiment on a real precision motion system. Finally, the conclusions and possible future work are discussed in Section 7.

2. Background

The optimization problem is given as (Sui et al., 2015a):

$$\min_{x \in A} g_0(x), \quad (1a)$$

$$\text{s.t. } g_j(x) \leq J_{\max}, \quad \forall j \in \{1, 2, \dots, J\}, \quad (1b)$$

where $x \in A \subset \mathbb{R}^n$ is a vector of decision variables from a continuous search space A , J_{\max} is the predefined constraint limit, $g_0 : \mathbb{R}^n \rightarrow \mathbb{R}$ is the objective function to be minimized and $g_j : \mathbb{R}^n \rightarrow \mathbb{R}$, $j = 1, \dots, J$ constraints that must be satisfied. It is assumed that the functional form of g_j , $j = 0, \dots, J$ is unknown, but we can get measurements of g_j that can be used to find surrogate models based on Gaussian processes.

2.1. Gaussian process regression

Following Berkenkamp et al. (2016), we use Gaussian processes to approximate g_j , $j = 0, \dots, J$, using measurements. We find approximations $\tilde{g}_j(x) : A \rightarrow \mathbb{R}$ where $j = 0$ corresponds to the objective function (1a), while $j = 1, \dots, J$ corresponds to the constraints (1b). Gaussian process regression, also called kriging, assumes that the values $\tilde{g}(x_0), \tilde{g}(x_1), \dots, \tilde{g}(x_P)$ corresponding to different x are random variables, with joint Gaussian distribution for any finite P . The prior information about the functions \tilde{g}_j is defined by known mean $\psi_j(\cdot)$ and covariance $k_j(\cdot, \cdot)$ functions:

$$\tilde{g}_j(x) \sim \text{GP}(\psi_j(x), k_j(x, x)), \quad (2)$$

We assume access to noisy measurements $\hat{g}_j(x) = g_j(x) + \omega$, $\omega \sim \mathcal{N}(0, \sigma_\omega^2)$. To use Gaussian processes corresponding to g_j in optimization, we need to predict the value of \tilde{g}_j at an arbitrary point \hat{x} using R past measurement

data $\mathbf{G}_j = [\hat{g}_j(x_r)]_{r=1,\dots,R}$. Following Rasmussen and Williams (2006), the mean and variance of the prediction at a new point \hat{x} are:

$$\mu_j(\hat{x}) = \psi_j(\hat{x}) + \mathbf{k}_R(\hat{x})(\mathbf{K}_R + \mathbf{I}_R\sigma_\omega^2)^{-1}(\mathbf{G}_j - \mathbf{\Psi}_j), \quad (3a)$$

$$\sigma_{R,j}^2(\hat{x}) = k(\hat{x}, \hat{x}) - \mathbf{k}_R(\hat{x})(\mathbf{K}_R + \mathbf{I}_R\sigma_\omega^2)^{-1}\mathbf{k}_R^\top(\hat{x}), \quad (3b)$$

where \mathbf{G}_j is a vector of R observed noisy values, $\mathbf{G}_j = [\hat{g}_j]_{j=1,\dots,R}$, $\mathbf{\Psi}_j = [\psi_j(x_r)]_{r=1,\dots,R}$ is a vector of mean values of the past data, $j = 0, \dots, J$, the matrix \mathbf{K}_R contains the covariance of past data, $k(x_a, x_b)$, $a, b = 1, \dots, R$, $\mathbf{k}_R(\hat{x})$ contains the covariance between the new point and the past data, and \mathbf{I}_R denotes identity matrix of dimension R .

The mean and the variance are then used to find the lower and upper confidence bounds:

$$l(x, j) = \mu_j(x) - \beta\sigma_{R,j}(x), \quad (4a)$$

$$u(x, j) = \mu_j(x) + \beta\sigma_{R,j}(x), \quad (4b)$$

where β corresponds to the desired confidence level.

2.2. SafeOpt

We follow the SafeOpt formulation from Sui et al. (2015a) with modifications proposed by Berkenkamp et al. (2016). The algorithm uses Gaussian processes as surrogates to solve the optimization problem (1). A set of safe points S_0 that fulfill (1b) is required for initialization. The safe set S_n at iteration n is:

$$S_n = \bigcap_{j \in \{1, 2, \dots, J\}} \{x \in A : u_n(x, j) \leq J_{\max}\}, \quad (5)$$

where $u_n(x, j)$ is the upper confidence bound of the Gaussian process that models the j -th constraint at point x at iteration n , obtained from (4b). The surrogate Gaussian processes are used to define the safe sets (5) after new samples are obtained in every iteration. Depending on the chosen β in (4), computing the safe set in iteration n can be used for risk assessment, quantifying the safety of points from the search space A (Azizoltani and Sadeghi, 2018).

To find the next iterate, SafeOpt defines the set of potential optimizers (minimizers) M_n :

$$M_n = \{x \in S_n : l_n(x, 0) \leq \min_{x \in S_n} u_n(x, 0)\}, \quad (6)$$

Table 1: Input for the auxiliary GP for the expanders, with the artificial observation to the right of the double line, if the current safe set contains a single point x^1 (adapted from Berkenkamp et al. (2016))

Inputs	x^1	x^1	x^1	\dots	x^1	\bar{x}	\bar{x}	\bar{x}	\dots	\bar{x}
Outputs	$g_0(x^1)$	$g_1(x^1)$	$g_2(x^1)$	\dots	$g_J(x^1)$	$l_n(\bar{x}, 0)$	$l_n(\bar{x}, 1)$	$l_n(\bar{x}, 2)$	\dots	$l_n(\bar{x}, J)$

with the lower bound $l_n(x, j)$ given in (4a). The set of points that can expand the current safe set (expanders) is defined as E_n (Sukhija et al., 2023):

$$E_n = \bigcup_{j=1}^J \{x \in S_n : |\mathcal{E}_j(x)| > 0\}, \quad (7)$$

where $|\mathcal{E}_j|$ is an indicator function describing if the set \mathcal{E}_j is non-empty:

$$\mathcal{E}_j(x) = \{x' \in A \setminus S_n : u_{n,j,(x,l_n(x,j))}(x') \leq J_{\max}\}. \quad (8)$$

Berkenkamp et al. (2016) defines $u_{n,j,(\bar{x},l_n(\bar{x},j))}(x')$ as the upper confidence bound of the point x' if \bar{x} was added to the GP with the evaluation $l_n(\bar{x}, j)$. The new auxiliary training dataset contains the previous dataset created from experiments and the upper bound of the previous GP evaluated at point \bar{x} from the current safe set as an artificial observation (Table 1, adapted from Berkenkamp et al. (2016)).

Using the sets of optimizers and expanders, the SafeOpt algorithm chooses to evaluate the point x_n according to:

$$x_n = \operatorname{argmax}_{x \in M_n \cup E_n} \max_j w_n(x, j) \quad (9a)$$

$$w_n(x, j) = u_n(x, j) - l_n(x, j) \quad (9b)$$

The iterations repeat until a termination criterion is met.

2.3. Grid-based SafeOpt

Grid SafeOpt relies on a discretization of the search space with a “grid”, $\mathcal{A} \subset A$. A summary of grid-based SafeOpt is shown in Algorithm 1. The sets from (5), (6), (7), which are necessary to solve (9a), are obtained in iteration n by doing an exhaustive search over the entire grid \mathcal{A} . If $|\mathcal{A}|$ is large, finding the sets \mathcal{E}_j in (8) for every point in S_n can be computationally expensive, because the auxiliary GP needs to be updated every time $u_{n,j,(x,l_n(x,j))}(x')$ is calculated (line 7 in Algorithm 1) (Berkenkamp et al., 2016).

Algorithm 1 Grid-based SafeOpt following Berkenkamp et al. (2016)

Require: A grid $\mathcal{A} \subset A$ with N points, initial safe set $S_0 = \{x^0, x^1, \dots, x^K\} \subset \mathcal{A}$, maximal number of iterations C , chosen β , desired safety threshold J_{\max}

- 1: Set $n \leftarrow 1$, compute $F_n = \{f(x^i)\}_{i=1, \dots, K}$, $G_{n,j} = \{g_j(x^i)\}_{i=1, \dots, K}$ for $j = 1, \dots, J$, set $S_n \leftarrow S_0$.
 - 2: **while** $n \leq C$ **do**
 - 3: Using S_n and F_n , find GP_f with lower bounds $l_n(x, 0)$, upper bounds $u_n(x, 0)$, from (4)
 - 4: Using S_n and $G_{n,j}$ find J $\text{GP}_{g,j}$ with lower bounds $l_n(x, j)$, upper bounds $u_n(x, j)$, from (4)
 - 5: Find $S_n \leftarrow \bigcap_{j \in \{1, 2, \dots, J\}} \{x \in \mathcal{A} : u_n(x, j) \leq J_{\max}\}$
 - 6: Using (6) find M_n
 - 7: For $j = 1, \dots, J$, for $\bar{x} \in S_n$, create $S_{n,\text{opt}} = S_n \cup \{\bar{x}\}$, $G_{n,j,\text{opt}} = G_{n,j} \cup l_n(\bar{x}, j)$.
 Using $S_{n,\text{opt}}$ and $G_{n,j,\text{opt}}$ find $\text{GP}_{g,j,\text{opt}}$ with upper bounds $u_{n,j}(\bar{x}, l_n(\bar{x}, j))$.
 - 8: For $j = 1, \dots, J$, for $x \in S_n$, $x' \in \mathcal{A} \setminus S_n$ evaluate $\mathcal{E}_j(x)$ to obtain E_n
 - 9: Solve (9a) to obtain x_n^r
 - 10: Set $n \leftarrow n+1$, $F_n \leftarrow F_{n-1} \cup \{f(x_n^r)\}$, $G_{n,j} \leftarrow G_{n-1} \cup \{g_j(x_n^r)\}$ for $j = 1, \dots, J$, $S_n \leftarrow S_{n-1} \cup \{x_n^r\}$
 - 11: **end while**
 - 12: **return** $x_C^r, f(x_C^r), S_C$
-

3. Grid-free SafeOpt

3.1. SafeOpt as a series of optimization problems

In grid-free SafeOpt from Zagorowska et al. (2023), the expanders E_n and minimizers M_n are found in the entire search space A , instead of being constrained by the grid \mathcal{A} . The search for the next iterate from (9a) is formulated as two optimization problems:

$$P_1 : \max_{x \in M_n \subset A} \max_j w_n(x, j) \quad (10)$$

$$P_2 : \max_{x \in E_n \subset A} \max_j w_n(x, j) \quad (11)$$

The new value x_n is obtained as the maximizing point from $E_n \cup M_n$:

$$x_n = \operatorname{argmax}_x \left\{ \max_{x \in E_n} w(x), \max_{x \in M_n} w(x) \right\}. \quad (12)$$

where $w(x) := \max_i w_n(x, i)$. To solve the problems P_1 and P_2 using numerical solvers, we rewrite the search space of each problem, M_n and E_n respectively, in the form of constraints. The grid-free algorithm is summarised in Algorithm 2.

Algorithm 2 Reformulated SafeOpt following Zagorowska et al. (2023)

Require: Initial safe set $S_0 = \{x^0, x^1, \dots, x^K\} \subset \mathcal{A}$, desired tolerances ϵ_1, ϵ_2 , maximal number of iterations C , chosen β , desired safety threshold J_{\max}

- 1: Set $n \leftarrow 1$, compute $F_n = \{f(x^i)\}_{i=1, \dots, K}$, $G_{n,j} = \{g_j(x^i)\}_{i=1, \dots, K}$ for $j = 1, \dots, J$, set $S_n \leftarrow S_0$.
- 2: **while** $n \leq C$ & $\|x_n^r - x_{n-1}^r\| \leq \epsilon_1$ & $\|f(x_n^r) - f(x_{n-1}^r)\| \leq \epsilon_2$ **do**
- 3: Using S_n and F_n , find GP_f with lower bounds $l_n(x, 0)$, upper bounds $u_n(x, 0)$,
- 4: Using S_n and $G_{n,j}$ find J $\text{GP}_{g,j}$ with lower bounds $l_n(x, j)$, upper bounds $u_n(x, j)$
- 5: Solve (16c), obtaining x_n^* and $l^* = l_n(x_n^*, 0)$
- 6: Solve P_1^j for all $j = 1, \dots, J$ from (16)
- 7: Solve P_2^j for all $j = 1, \dots, J$ from (26)
- 8: **if** $q_j(x_2^{j*}, x_1^*) \geq w_n(x_2^{j*}, j)$ **then**
- 9: Solve (30) and set $x_n^r \leftarrow \arg \max_{\{x_1^*, x_2^*\}} \{w_n(x_2^*, k_2^*), w_n(x_1^*, k_1^*)\}$
- 10: **else**
- 11: Set $x_n^r \leftarrow x_1^*$
- 12: **end if**
- 13: Set $n \leftarrow n+1$, $F_n \leftarrow F_{n-1} \cup \{f(x_n^r)\}$, $G_{n,j} \leftarrow G_{n-1} \cup \{g_j(x_n^r)\}$ for $j = 1, \dots, J$, $S_n \leftarrow S_{n-1} \cup \{x_n^r\}$
- 14: **end while**
- 15: **return** $x_n^r, f(x_n^r), S_n$

3.1.1. Minimizers

From the definition of the safe set from (5), we obtain that:

$$x \in S_n \iff x \in A \text{ and } \forall j = 1, \dots, J \quad u_n(x, j) \leq J_{\max}. \quad (13)$$

From the definition of the minimisers (6) we obtain:

$$x \in M_n \iff x \in S_n \text{ and } l_n(x, 0) \leq l^*, \quad (14)$$

where:

$$l^* = \min_z u_n(z, 0), \quad (15a)$$

$$\text{subject to } u_n(z, j) \leq J_{\max}, \quad \forall j = 1, \dots, J. \quad (15b)$$

We note in (10) that $w_n(\cdot, i)$, $w_n(\cdot, j)$ are independent from each other for $i \neq j$. Therefore, the objective function (10) can be reformulated into J separate problems P_1^k , $k = 1, 2, \dots, J$. Using (13) and (14), the minimizer

problem (10) becomes:

$$P_1^k : \max_{x \in A} w_n(x, k), \quad (16a)$$

$$\text{subject to: } u_n(x, j) \leq J_{\max} \quad \forall j \in \{1, 2, \dots, J\}, \quad (16b)$$

$$l_n(x, 0) \leq \min_{\hat{x} \in S_n} u_n(\hat{x}, 0). \quad (16c)$$

The solution to (10) is then:

$$x_1^* = \operatorname{argmax}_{k \in \{1, 2, \dots, J\}} w_n(x_1^{k*}, k) \quad (17)$$

where x_1^{k*} is the solution to (16).

3.1.2. Expanders

Combining (11) and (7) we get:

$$\max_x \max_i w_n(x, i), \quad (18a)$$

$$\text{subject to } x \in S_n, \quad (18b)$$

$$|\mathcal{E}(x)| > 0, \quad (18c)$$

where $\mathcal{E}(\cdot)$ is given by (8). From (8) we notice that the set $\mathcal{E}(x)$ is non-empty if there exists at least one point $x' \in A \setminus S_n$ such that the condition:

$$\forall j \ u_{n,j,(x,u_n(x,j))}(x') \leq J_{\max} \quad (19)$$

is satisfied. Thus, we obtain:

$$\max_{x, x'} \max_i w_n(x, i), \quad (20a)$$

$$\text{subject to } x \in S_n, \quad (20b)$$

$$u_{n,j,(x,u_n(x,j))}(x') \leq J_{\max}, \quad \forall j = 1, \dots, J, \quad (20c)$$

$$x' \in A \setminus S_n. \quad (20d)$$

From the definition of the safe set (5), we get that:

$$x' \in A \setminus S_n \iff x' \in A \text{ and } \exists k : u_n(x', k) > J_{\max}. \quad (21)$$

Then we have the following equivalence:

$$\exists k : u_n(x', k) > J_{\max} \iff \max_s u_n(x', s) > J_{\max}, \quad (22)$$

from which we obtain:

$$\max_{x,x'} \max_i w_n(x, i), \quad (23a)$$

$$\text{subject to } \max_s u_n(x, s) \leq J_{\max}, \quad (23b)$$

$$\max_s u_n(x', s) > J_{\max}, \quad (23c)$$

$$\max_s u_{n,s,(x,u_n(x,s))}(x') \leq J_{\max}. \quad (23d)$$

$$(23e)$$

The constraint (23c) is feasible if $S_n \subsetneq A$. The constraint (23d) may be infeasible if the set of expanders G_n is empty (Berkenkamp et al., 2016). To avoid infeasibility, we relax (23):

$$\max_{x,x'} q(x, x'), \quad (24a)$$

$$\text{subject to } \max_s u_n(x, s) \leq J_{\max}, \quad (24b)$$

$$\max_s u_n(x', s) > J_{\max}, \quad (24c)$$

where:

$$q(x, x') = \max_i w_n(x, i) - \sigma \max\{0, \max_s u_{n,s,(x,l_n(x,s))}(x') - J_{\max}, \} \quad (25)$$

and $\sigma > 0$ enables trading off feasibility and optimality. The relaxation in (25) has been introduced to ensure the feasibility of (11) in the case the expanders do not exist while preserving the measurement-based nature of (8) introduced by Berkenkamp et al. (2016). If σ is too small, the optimization may return an infeasible point. Conversely, choosing a large σ puts emphasis on feasibility, at the expense of finding the optimum.

Doing the same reformulation as in (16), we get the expander problem (11) formulated as a series of J problems:

$$P_2^k : \max_{x,x' \in A} q_k(x, x'), \quad (26a)$$

$$\text{subject to: } \max_{j \in \{1,2,\dots,J\}} u_n(x, j) \leq J_{\max}, \quad (26b)$$

$$\max_{j \in \{1,2,\dots,J\}} u_n(x', j) > J_{\max}, \quad (26c)$$

with:

$$q_k(x, x') = w_n(x, k) - \sigma \max\{0, \max_j u_{n,j,(x,l(x,j))}(x') - J_{\max}\}. \quad (27)$$

If we denote the solution of (26) $(x_2^{k*}, x_2'^{k*})$, the solution to (11) is defined as:

$$x_2^* = \operatorname{argmax}_{k \in \{1, 2, \dots, J\}} w_n(x_2^{k*}, k). \quad (28)$$

To consider the solution x_2^* in (28) to be an expander, it is now necessary to check the gap between $q(x_2^*, x_2'^*)$ from (25) and $\max_i w_n(x_2^*, i)$ from (23). If, for every j , x_2^* and $x_2'^*$ fulfill:

$$q_j(x_2^*, x_2'^*) \geq w(x_2^*, j), \quad (29)$$

then the algorithm chooses x_n between x_1^* and x_2^* by solving:

$$x_n = \operatorname{argmax}_{\{x_1^*, x_2^*\}} \{w_n(x_1^*, k_1^*), w_n(x_2^*, k_2^*)\}. \quad (30)$$

If (29) is not satisfied, then $u_{n,j,(x,l(x,j))}(x') > J_{\max}$ and $x_n = x_1^*$.

The problems (16), (26) use the same definitions of the optimizers and the expanders as Berkenkamp et al. (2016), thus preserving the safety properties of SafeOpt (Berkenkamp et al., 2021).

4. Embedding numerical solvers in SafeOpt

4.1. Initialization

To facilitate the solution of (10) and (11) with local solvers, we first propose an initialization method. Let us recall that we assume some initially feasible safe set S_0 . Optimization problems (16c) and subsequently (16) (lines 5 and 6 in Algorithm 2) are feasible for all $x \in S_n$, $n \geq 0$. Thus, starting the local solver with an initial guess $\hat{x} \in S_n$ ensures that a feasible solution exists. We choose to start the optimization problems at the current best solution, $\hat{x} = \operatorname{argmin} F_n$ where $F_n = \{f(x^i)\}_{i=1, \dots, K}$ contains the values of the objective function evaluated at the samples x^i obtained until iteration n (line 1 in Algorithm 2).

To overcome the limitations of using a local solver, we use the definition of the safe set (5) to find an initial guess for the expander search (26). Starting a local solver from infeasible points can lead to only finding points that do not fulfill (26c) in (26). Following Duivenvoorden et al. (2017) and König et al. (2021), we look for expanders on the boundary of the current safe set.

The proposed procedure to generate a feasible starting point for the search is summarised in Algorithm 3. We sample m points x_i from S_n (line 1) and

Algorithm 3 Generating starting points for (26)

- 1: Generate m safe points x_i from S_n , $i \in \{1, 2, \dots, m\}$
 - 2: Generate l unsafe points x'_j from $A \setminus S_n$, $j \in \{1, 2, \dots, l\}$
 - 3: Calculate the Euclidean distance between each safe and unsafe point and store them in a matrix $M \in \mathbb{R}^{m \times l}$
 - 4: **for** $i \in \{1, 2, \dots, m\}$ **do**
 - 5: Find $j^* \leftarrow \underset{j \in \{1, 2, \dots, l\}}{\operatorname{argmin}} M_{ij}$
 - 6: Create potential starting points $\hat{x}_i \leftarrow [x_i, x'_{j^*}]$
 - 7: **end for**
 - 8: **return** $\{\hat{x}_i\}_{i=1, \dots, m}$
-

l points x'_j from $A \setminus S_n$ (line 2) in every iteration. Choosing a combination of safe and unsafe points as a starting point gives feasibility of (11). To find points at the boundary of the current safe set, we look at the Euclidean distance between points chosen from S_n and $A \setminus S_n$ (line 3). The points in the safe set and in the unsafe set are paired up according to the minimal Euclidean distance between them, i.e. each of m safe points is paired up with the unsafe point closest to it (lines 4-7). The procedure returns a set of m pairs, $\{\hat{x}_i\}_{i=1, \dots, m}$ where $\hat{x}_i = [x_i, x'_{j^*}]$.

Algorithm 3 provides a set of feasible points $\{\hat{x}_i\}_{i=1, \dots, m}$. We choose one point from $\{\hat{x}_i\}_{i=1, \dots, m}$ as a starting point to solve (26). We also note that multiple initial guesses can be considered in parallel.

4.2. Choice of solver

The proposed reformulation is independent of the chosen optimization solver. We focus on derivative-free methods to preserve the derivative-free character of Bayesian optimization. Zagorowska et al. (2023) explored the flexibility provided by using pattern search methods to introduce new stopping criteria for the reformulated SafeOpt algorithm. Pattern search methods belong to the group of direct search optimization methods and rely on evaluating a number of candidate points around a selected point, which are chosen from a *mesh* following a given *pattern*. The mesh can be intuitively understood as local discretization of adjustable size around the current point. If the size of the mesh falls below a given threshold, the algorithm stops. Audet and Hare (2017) provide an in-depth description of the algorithm and its convergence properties.

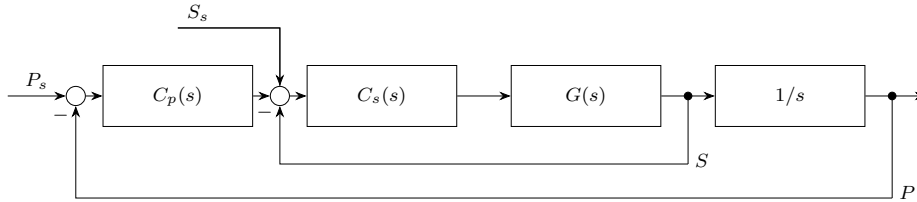


Figure 1: Block diagram of a ball-screw drive with transfer function $G(s)$. The objective is to follow the position set point P_s ensured by a proportional controller $C_p(s)$ in cascade with a speed controller $C_s(s)$ (adapted from Zagorowska et al. (2023))

5. Controller tuning with unknown constraints

5.1. Simulation setup

To test the proposed reformulation of SafeOpt, we first show results from a numerical simulation of tuning a cascade PID controller for the ball-screw drive from Khosravi et al. (2020) and Zagorowska et al. (2023) (Fig. 1). The objective is to find a parameter K_p for the position controller $C_p(s)$ and the parameters K_v and K_{vi} for the speed control $C_s(s)$ to minimize weighted average in the position error $P - P_s$ and the speed error S :

$$J := \gamma_1 \|P - P_s\|_1 + \|S\|_\infty. \quad (31)$$

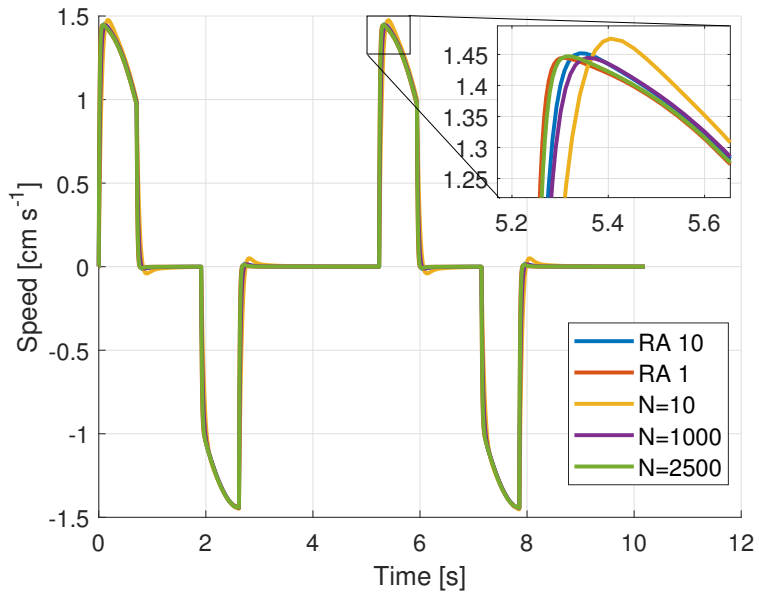
To put emphasis on tracking the desired position setpoint P_s in this example, we set $\gamma_1 = 1000$ in accordance with the magnitude of the measured signals.

To emulate human-driven PID tuning based on visual assessment of responses of the system (Åström and Hägglund, 2006, Ch. 4.4), we measure stability as the slope p_1 of the peaks of the response of the system, with positive values indicating instability. The constraint was formulated as:

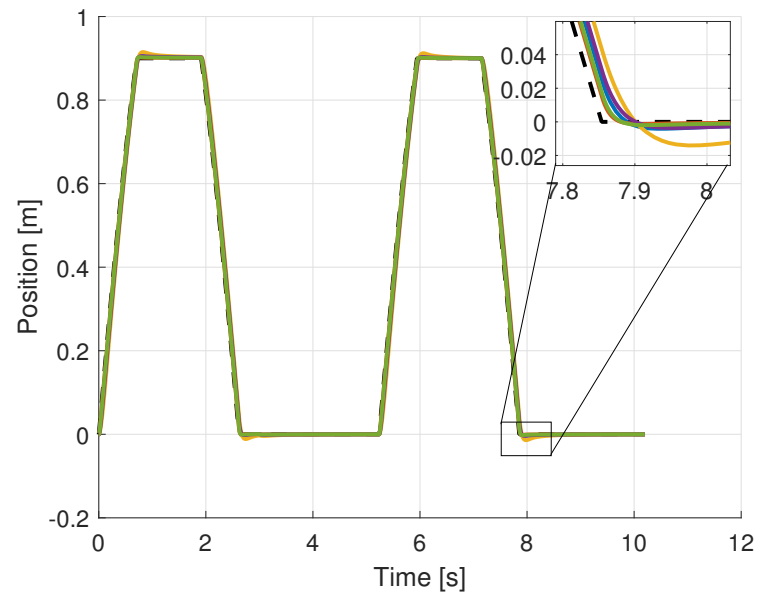
$$h(K_p, K_v, K_{vi}) := \gamma_2(p_1 - \sigma) \leq 0, \quad (32)$$

where $\gamma_2 = 100$ for scaling and $\sigma = 0.005$ was chosen to ensure that a system with no peaks, i.e. $p_1 = 0$, yields a value inside the feasible set.

Setting $x := [K_p, K_v, K_{vi}]^\top$, we obtain the problem structure of (1). The search space $\mathcal{A} = [0, 110] \times [0, 50]^2$ was chosen so that it contains unstable values. The initial safe set contains four points found using the simulation. Table 2 shows the values of the objective (31) and the constraint (32) for the initial safe set S_0 and $J_{\max} = 0$. For the simulations, we used squared exponential kernels with hyperparameters obtained using `fitrgp` in Matlab (Zagorowska et al., 2023).



(a) Speed



(b) Position

Figure 2: Speed and position for the truncated sinusoidal position set point

Table 2: The initial safe set S_0 , and an unsafe point, with the corresponding value of the objective function and the constraint (adapted from Zagorowska et al. (2023))

	K_p	K_v	K_{vi}	Obj. (31)	Cstr. (32)
Unsafe point	30	0	5	388	4.6
Safe point I	10	0	5	241	-4.8
Safe point II	20	0.4	50	20	-5.4
Safe point III	42	0.3	12	39	-5.8
Safe point IV	90	0.5	1	26	-0.005

5.2. Performance of grid-free SafeOpt

All tests in this section were performed in Windows 10, using Matlab 2022a on a laptop with an AMD Ryzen 7 PRO 5850U, 8 cores, with 32 GB of RAM. The model of the controller from Fig. 1 was developed in Simulink version 2022a, update 5.

Following the performance comparison from Zagorowska et al. (2023), the parameters of the reformulated algorithm were chosen as $\epsilon_1 = \epsilon_2 = 0.1$, with a mesh tolerance of 0.01 and the initial mesh sizes of 10 (RA 10) and one (RA 1). A comparison with grid-based SafeOpt for three grids with $N \in \{10, 1000, 2500\}$ is shown in Fig. 2. The position trajectory P_s was a sinusoidal function, truncated at 0.9 and zero (dashed black in Fig. 2b). The best results in terms of both the objective and the computational time (value 3.4 obtained for 17 s) were obtained for the grid-free version of SafeOpt with the initial mesh size equal to one (orange). The default SafeOpt was second best in terms of the objective (green line), at the expense of the computational time (value of 4.3, obtained in 56 s).

5.3. Impact of initialization

All tests in this section were performed in Windows 11 Pro, using Matlab 2022a on a laptop with an 11th Gen Intel(R) Core(TM) i7-1165G7 processor, with 32 GB of RAM. The model of the controller from Fig. 1 was developed in Simulink version 2022a, update 5.

To further analyse the performance of the reformulation from Section 3.1, we implemented Algorithm 3 in the simulation setup. The performance was evaluated from the perspective of the timings for solving (11), averaged over ten runs, and the resulting safe set after the algorithm has converged. The stopping criteria for SafeOpt were $\epsilon_1 = \epsilon_2 = 0.1$, and for pattern search

Table 3: Timings of implementation of Algorithm 3 to generate an initial guess for expander search (first four rows), together with a fixed unstable point from Table 2 used as a guess for x' (last row), using Latin hypercube sampling (LH) and random sampling (R)

m_0	Resulting safe set [%]	Time [s] for Algorithm 3	Time [s] for solving (11)	Overall time [s]
100	31 $LH R$ 28	0.00087 $LH R$ 0.00086	0.04 $LH R$ 0.05	2.9 $LH R$ 3.7
300	5 $LH R$ 76	0.0009 $LH R$ 0.001	0.04 $LH R$ 0.06	2.4 $LH R$ 2
500	15 $LH R$ 35	0.0014 $LH R$ 0.0011	0.03 $LH R$ 0.03	2.5 $LH R$ 2.4
700	0.3 $LH R$ 5	0.0012 $LH R$ 0.0014	0.03 $LH R$ 0.05	3 $LH R$ 2.73
-	28	n/a	10	27

constraint tolerance $\varepsilon = 0.01$, and minimum mesh size $\delta^0 = 1$. We used two kinds of sampling from the search space A in Algorithm 3: Latin hypercube sampling from Iman and Shortencarier (1984) (using `lhsdesign`) and random sampling (using `rand`). The m safe points were obtained by evaluating (5) for the m_0 points. The number of unsafe points was then $l = m_0 - m$. We chose $m_0 \in \{100, 300, 500, 700\}$ (rows 2-5 in Table 3) and paired it with a fixed unstable point from Table 2 used as a guess for x' in the expander search (top row in Table 2).

5.3.1. Impact on timing

Algorithm 3 was implemented by first sampling m_0 points from the search space using Latin hypercube sampling. The results of running the Algorithm 2 with Algorithm 3 used for starting the expander search are shown in Tables 3 and 4. In all the cases, the reformulated SafeOpt needed $T = 4$ iterations, and all iterations have found expanders. The results from all the cases were also close, with the objective function 5.69, the parameters $K_p = 62$, $K_v = 32.36$, $K_{vi} = 50$ if Algorithm 3 was used and 5.64 the parameters $K_p = 62.25$, $K_v = 32.38$, $K_{vi} = 50$ if the starting point was fixed.

The impact of using Algorithm 3 is primarily visible in the timing for solving the expander search (11), which is then propagated to the overall time (columns 3 and 4 in Table 3, respectively). Starting the expander search from a fixed initial point required nine times as long as starting on the boundary of the current safe set. The initialization based on generating and evaluating m_0 points in Algorithm 3 is thus faster than starting the optimization problem from a fixed point. Moreover, the overall time for SafeOpt using Algorithm 3 remains similar regardless of m_0 .

Table 4: Results of implementation of Algorithm 3 to generate an initial guess for expander search (first four rows), together with a fixed unstable point from Table 2 used as a guess for x' (last row), using Latin hypercube sampling (LH) and random sampling (R)

m_0	T	# iterations with expanders	K_p^*	K_v^*	K_{vi}^*	Objective
100	4 $LH R$ 4	4 $LH R$ 4	62 $LH R$ 62	32.36 $LH R$ 32.36	50 $LH R$ 50	5.7 $LH R$ 5.7
300	4 $LH R$ 2	4 $LH R$ 2	62 $LH R$ 20	32.36 $LH R$ 0.36	50 $LH R$ 50	5.7 $LH R$ 20
500	4 $LH R$ 4	4 $LH R$ 4	62 $LH R$ 62	32.36 $LH R$ 32.36	50 $LH R$ 50	5.7 $LH R$ 5.7
700	4 $LH R$ 4	4 $LH R$ 3	62 $LH R$ 62	32.36 $LH R$ 32.36	50 $LH R$ 50	5.7 $LH R$ 5.7
-	4	4	62.25	32.38	50	5.6

The impact of the starting guesses in solving (11) is visible if random sampling was used in Algorithm 3. Choosing $m_0 = 300$ by using random sampling resulted in points that made finding an improved solution impossible. In particular, in the first iteration of SafeOpt, the recommended value from (30) was chosen as a minimizer from the initial safe set in Table 2. As we assumed no noise in the simulation, the new measurement obtained from applying the recommended value was identical to a measurement corresponding to the safe point. Thus, it triggered the stopping criterion defined by ϵ_2 and the algorithm stopped. The resulting controller parameters are selected as one of the initial safe points (second row in Table 4) and the corresponding value of the minimized objective function is large (last column in Table 4). Even though the case with no noise is rarely encountered in practice, a possible remedy is to use the number of iterations as a stopping criterion at the expense of increased time.

5.3.2. Impact on safe sets

The performance of using Gaussian processes as surrogates to quantify safety depends on the sampled points used in computation of (3a) and (3b). From (30), we see that the sets of expanders and optimizers define the sample in iteration $T - 1$, thus affecting the safe set S_T in iteration T . We use the safe set S_T to quantify the impact of Algorithm 3 on grid-free SafeOpt by evaluating (5) for 500000 points sampled from the entire search space using Latin hypercube sampling from Iman and Shortencarier (1984).

The impact of m_0 in Algorithm 3 is visible in the resulting safe set (second column in Table 3). If $m_0 = 100$, the final set of parameters considered safe covered a third of the entire search space. Conversely, choosing $m_0 = 700$ led to a safe space of 0.3% (magenta in Fig. 3). Figure 3 shows that for 100

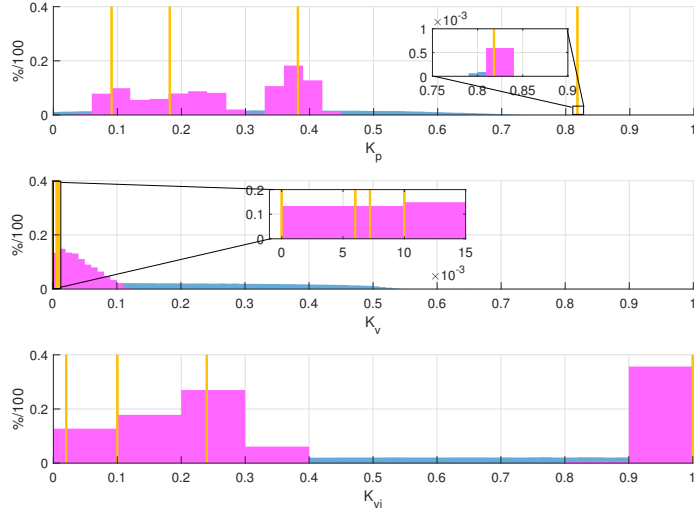


Figure 3: (Color online) The final safe set obtained from SafeOpt if Algorithm 3 was used with $m_0 = 100$ (blue) and $m_0 = 700$ (magenta) points. The initial safe set S_0 is marked with yellow

points, the region of the search space covered for 100 points is large (blue in Fig. 3). This is because the initial guess for the expander search was farther from the initial safe set. Conversely, the final safe set obtained for 700 points (magenta) is clustered around the initial safe set (yellow circles). The clustering is especially prominent in the case of K_v (middle plot). The clustering is due to the choice of the value of K_v in the initial set close to zero (third column in Table 2). The expanders remained close to zero because the local search was started close to the initial safe set thanks to 700 points.

Figures 4 and 5 show a comparison of the safe set obtained for 100 points if the Latin hypercube sampling was used with a fixed initial guess (black in Fig. 4) and with a random sampling (light green in Fig. 5). In all the cases, the safe sets cover a similar part of the search space, around 30% (first and last row in Table 3). The main difference is in the time necessary to find a solution (last column in Table 3). The algorithm proposed in the paper allows obtaining the same safe set while being faster. Using Latin hypercube sampling allows better coverage of the search space, leading to a speed-up of 0.8 s compared to random sampling. Thus, the analysis of the safe sets indicates that there is potential in exploiting the initial point for the

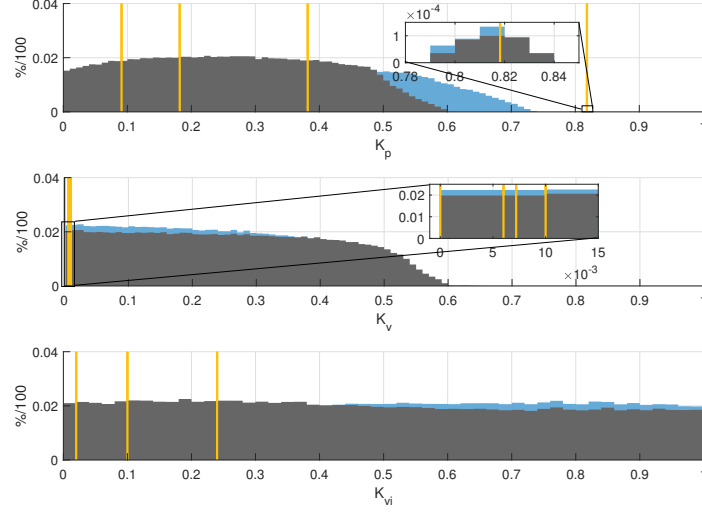


Figure 4: (Color online) The final safe set obtained from SafeOpt if Algorithm 3 was used with $m_0 = 100$ (blue) and if a fixed starting point for the expander search was used (black). The initial safe set S_0 is marked with yellow

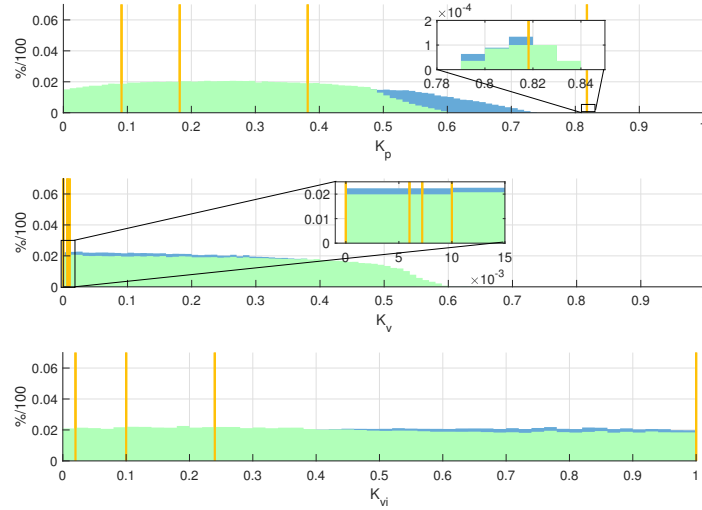


Figure 5: (Color online) The final safe set obtained from SafeOpt if Algorithm 3 was used with $m_0 = 100$ generated with Latin hypercube sampling (blue) and with random sampling (light green). The initial safe set S_0 is marked with yellow

expander search by adjusting both m_0 and the sampling method, to provide risk assessment with respect to parameters of the chosen controller.

6. Optimization of the control parameters of a high-precision motion system

The experimental validation of the proposed grid-free SafeOpt was done by tuning the controller gains of a high-precision motion system (motion stage) from Schneeberger Linear Technology (Rothfuss et al., 2022). The system is shown in Fig. 6 and consists of a 2D positioning stage with two orthogonal linear axes (pink and blue) and one rotational axis (yellow), though here we only consider the motion along the upper linear axis (blue). The axis is driven by a permanent magnet AC motor with precision encoders for position and speed tracking. The positioning accuracy of the axis is below $10 \mu\text{m}$, with repeatability below $0.7 \mu\text{m}$, and 3σ stability below 1 nm . The system is controlled by a cascade controller with a proportional controller (P) for the position and a proportional-integral (PI) controller for the velocity (Fig. 7) that should be tuned to achieve sub-micrometer precision (Lee et al., 2000). Following König et al. (2023) we use a sampling time of the controller and the data acquisition of the system of 2.5 kHz . The buffer length of each measurement is 3000 points, which results in a 1.2 s measurement for each step. The performance of the system is given by the filtered average position error over the 1.2 s measurement.

The results of SafeOpt in grid-based and grid-free version were compared to the gains of the automatic tuner that is built into the controller and the benchmark algorithm (Goal-oriented Safe Exploration) GoOSE developed by König et al. (2021), adapted for continuous, adaptive controller tuning in precision motion systems by König et al. (2023). GoOSE ensures that every input to the system satisfies an unknown, observable constraint. For controller tuning, it unifies time-varying Gaussian process bandit optimization from Bogunovic et al. (2016) with multi-task Gaussian processes from Swersky et al. (2013), and with efficient safe set search based on particle swarm optimization as introduced in König et al. (2023).

6.1. Controller tuning problem

The gains of the controller are the proportional position gain (PKP), the proportional velocity gain (VKP), the integral velocity gain (VKI), and the feedforward gain of the acceleration (AFF). The step size α , which is the

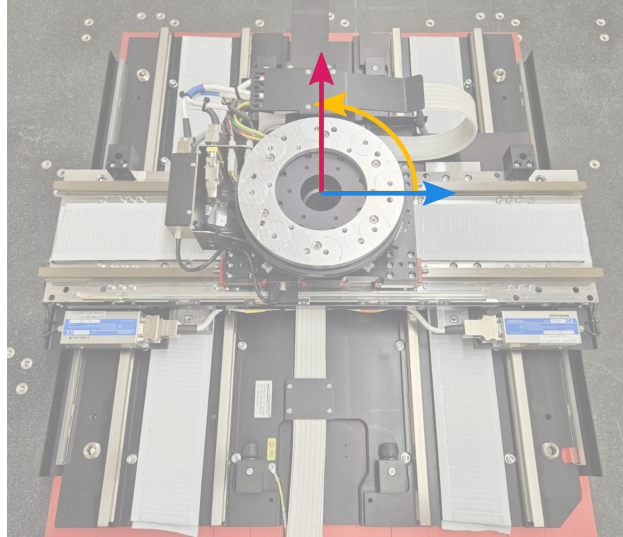


Figure 6: High precision motion system with the two linear axes (lower (pink), and upper (blue) that is considered in this work), and the rotational axis (yellow)

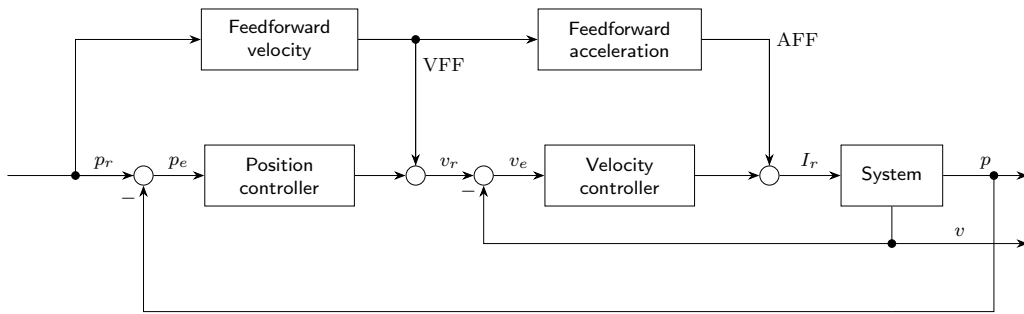


Figure 7: Simplified block diagram of the controller. The signals p_r, v_r, I_r are the reference signals of position, velocity and current respectively, p_e, v_e are the position and velocity error signals from which the objective and constraint features are calculated, while p and v are the actual position and velocity. The signals VFF and AFF are feedforward signals to the velocity and acceleration cycle of the cascaded controller. The block “Position controller” is a proportional controller with parameter PKP, the “Velocity controller” is a proportional-integral (PI) controller with parameters VKP and VKI, the velocity feedforward gain is fixed, $VFF=1$, while the acceleration feedforward gain AFF is tuned

distance the system covers in one motion, was a task parameter as described by König et al. (2021). The goal was to minimize the average position error for one linear axis, and a constraint was put on the fast Fourier transform of the velocity error e_v and the average position error. The optimization problem is formulated as:

$$\min_{x \in A} e_{\text{avg}}(x), \quad (33a)$$

$$\text{subject to: } e_{\text{avg}}(x) \leq J_{\text{max}}^1(\alpha), \quad (33b)$$

$$\max_{f \in [140\text{Hz}, 1250\text{Hz}]} |\text{FFT}[\xi(i, n_s)v_e(t_i)](x)| \leq J_{\text{max}}^2(\alpha) \quad (33c)$$

where:

$$e_{\text{avg}}(x) := \frac{1}{n_P - n_s} \sum_{i=n_s}^{n_P} |\xi(i, n_s)p_e(t_i)|. \quad (34)$$

The position and velocity error p_e and v_e depend on the controller parameters, x is a vector with the four gains and the stepsize [PKP, VKP, VKI, AFF, α] and J_{max}^1 and J_{max}^2 are the constraint limits which depend on the stepsize α . The search space is defined as $A = [100, 450] \times [450, 1500] \times [800, 2500] \times [0, 2]$, and $\xi(i, n_s)$ is the right-sided sigmoid filter function

$$\xi(i, n_s) = 1 - (1 + \exp(-(i - n_s - 150)/10))^{-1}.$$

Finally, n_s is the time sample where the movement of the position reference function ends and the sampling time begins, while n_P is the time sample of the end of the settling time set at 1.2 s after start of the movement.

6.2. Results

All learning algorithms, grid SafeOpt, grid-free SafeOpt, and GoOSE, used Gaussian processes to model (33b) and (33c) with a squared exponential kernel with the lengthscales: $l_{\text{PKP}} = 50$, $l_{\text{VKP}} = 100$, $l_{\text{VKI}} = 200$, l_{AFF} and $l_{\text{stepsize}} = 0.3$. The variance of the kernel for e_{avg} was set to 0.36×10^{-10} and for FFT_{max} to 1×10^{-4} . We set $\beta = 3$ in (4), as in practice choosing $\beta \geq 2$ often proves sufficient (König et al., 2021). The number of points in Algorithm 3 was set $m = 300$, and the samples were obtained using Latin hypercube sampling. The stopping criterion for all the algorithms was set to 100 iterations. As the local solver algorithm we chose a custom implementation of Generalised Pattern Search from Audet and Hare (2017) in Python 3.9. The tests were run on a Dell Inc. Precision 5820 Tower PC with 64 GB RAM.

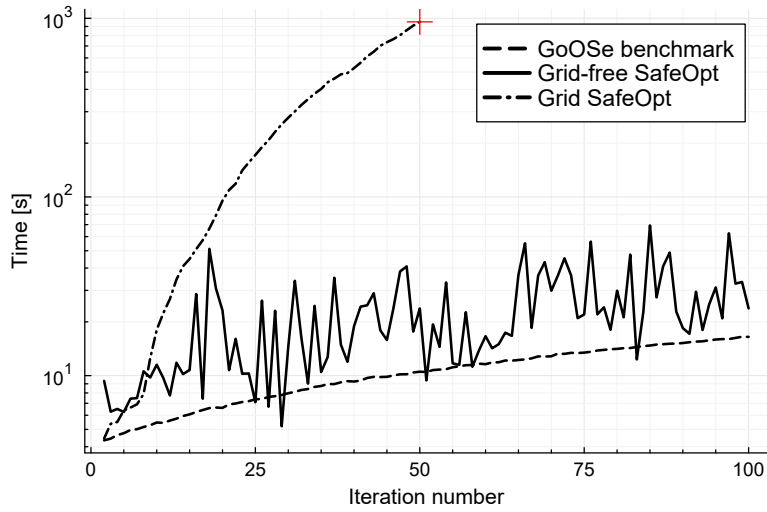
The runtime of a single iteration is shown in Fig. 8a. While the iteration times for both SafeOpt algorithms start around 10 s, the iteration time of grid SafeOpt grows much faster than grid-free SafeOpt. As a result, grid SafeOpt was interrupted after 4 hours (50 iterations) since iteration times reached 20 minutes per iteration. Conversely, an iteration of grid-free SafeOpt performs similarly to the benchmark GoOSE. Thus, grid-free SafeOpt and GoOSE were run for 100 iterations taking 37 and 18 minutes, respectively. The difference in timings between GoOSE and grid-free SafeOpt arises because GoOSE focuses on evaluating the optimizers, limiting the use of expanders and thus removing the computation of the auxiliary GPs from (9a).

Figure 8b shows the iteration times broken down into the optimizer search time and the expander search time. For both SafeOpt algorithms, most of the iteration time is taken up by the expander search. The time for the optimizer search is similar for both. The long search times for expanders stems from the calculation of $u_{n,j,(x,l_n(x,j))}(x')$ since this is done by adding and removing $(x, l_n(x, j))$ from the GPs. The computational cost grows with the number of evaluations added to the auxiliary GPs (line 7 in Algorithm 1). Therefore, the cost also grows with the number of iterations, since an evaluation is added in every iteration. In grid SafeOpt these calculations have to be done for every safe point in the entire grid, leading to a long runtime. In grid-free SafeOpt the calculation of necessary to find \mathcal{E}_j in the expander search is only done for the points pattern search chooses to evaluate. As a result, the time for a single iteration in grid-free SafeOpt remains similar over time.

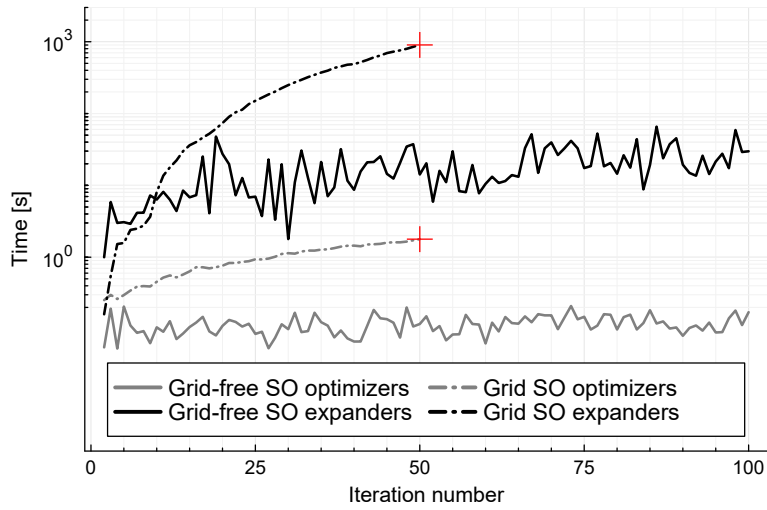
The points evaluated by the three algorithms are shown in Fig. 9. Both SafeOpt algorithms are searching in the same part of the search space, but grid SafeOpt (triangles) evaluates points that are on a grid while the points selected by grid-free SafeOpt (squares) are less restricted. Grid-free SafeOpt finds points with a smaller e_{avg} compared to grid SafeOpt (Fig. 10). This is because grid SafeOpt is restricted to the grid and thus unable to find a better point that lies between points of the grid. Finally, as GoOSE computes only optimizers, the values of the parameters are less spread across the search space. Grid-free SafeOpt explores a wider part of the search space, at the expense of increased computational time.

6.3. Comparison with automatic tuner and GoOSE

Table 5 shows the predicted optimal gains and the resulting average position error for grid SafeOpt, grid-free SafeOpt, and GoOSE. Grid-free SafeOpt predicted a better optimum than grid SafeOpt within the given timeframe.



(a) The iteration times for grid SafeOpt (dash-dotted) and grid-free SafeOpt (solid), compared to the benchmark GoOSE (dashed)



(b) The iteration times for expanders (black) and optimizers (gray) from grid SafeOpt (dash-dotted) and grid-free SafeOpt (solid)

Figure 8: Time comparison

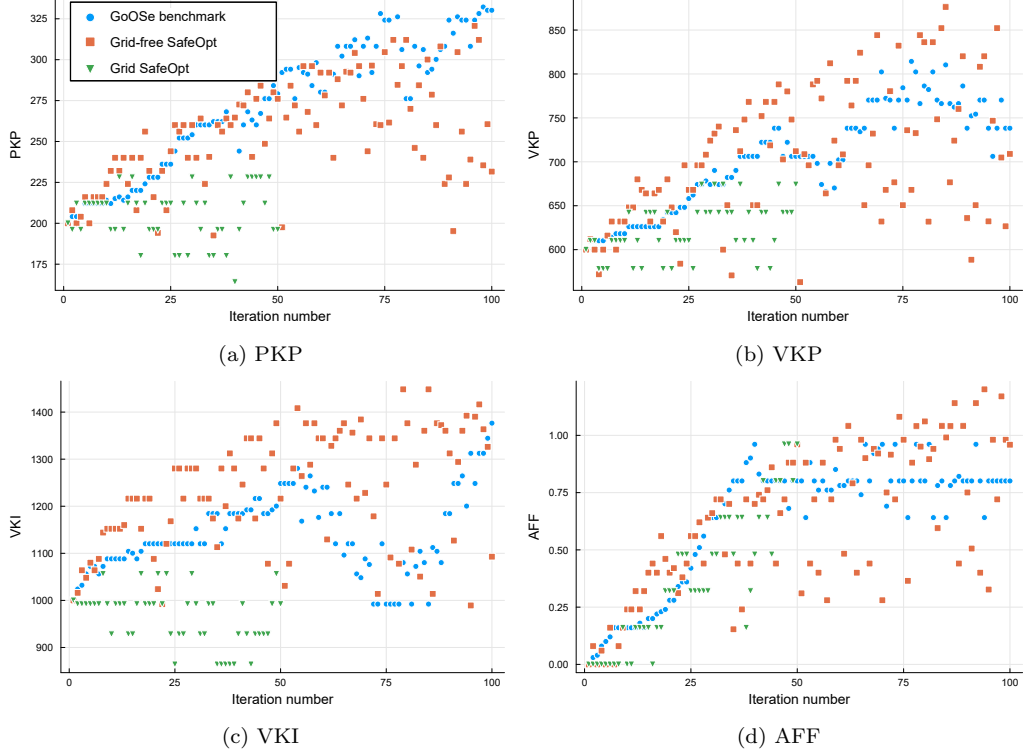


Figure 9: Comparison of the evaluated points from grid SafeOpt (triangles) and grid-free SafeOpt (squares) with the benchmark solution from GoOSE (circles)

Table 5: Comparison of grid-free SafeOpt with grid SafeOpt, automatic tuning, and benchmark GoOSE using a 10 mm step on 10 different positions on the motion stage, and the mean and standard deviation of the cost over the 10 repetitions over the positions are included. The superscript ⁺ indicates that the solution was interrupted after 50 iterations. The cost is uniformly scaled by 10^{-7} for presentation

Algorithm	Solution $x^* = [\text{PKP}, \text{VKP}, \text{VKI}, \text{AFF}]$	Scaled Cost (33a)	Runtime [min]
Grid SafeOpt	[212.1, 546.1, 800, 0.961]	136.7 ± 8.81	253 ⁺
Grid-free SafeOpt	[304.1, 836.2, 1440.4, 0.841]	23.29 ± 3.44	37
Autotuning	[350, 600, 2000, 0]	52.63 ± 4.15	2
GoOSE	[332.2, 746.3, 1344.5, 0.741]	31.65 ± 3.98	18

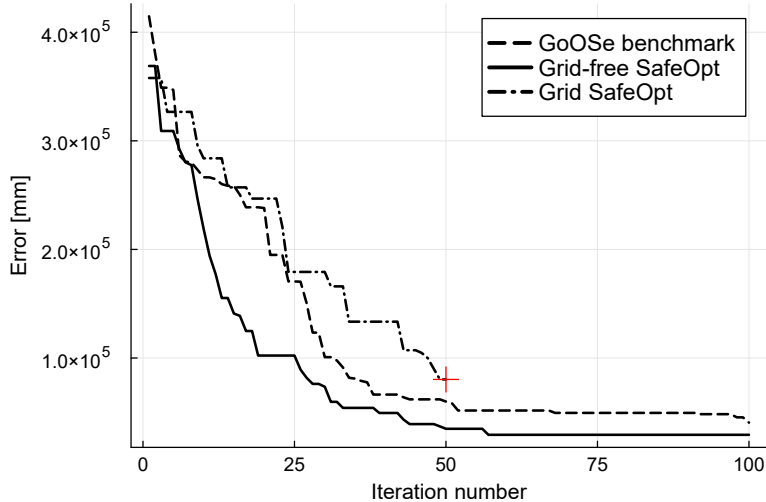


Figure 10: Comparison of the smallest e_{avg} as a function of iteration for grid SafeOpt (dash-dotted), grid-free SafeOpt (solid), and the benchmark GoOSE (dashed)

Figure 10 shows that grid-free Safeopt evaluates points with a smaller average position error than grid SafeOpt. The proposed grid-free algorithm also achieves performance 30% better than GoOSE, thanks to using expanders as well as optimizers and exploring a larger part of the search space.

Figure 11 shows the average position error for the four different configurations of the controller from Table 5. The four controllers were validated for 10 different set-points and the average error is shown in Fig. 11. All four algorithms drive the error towards zero. In particular, the proposed grid-free SafeOpt (solid) has better performance with the benchmark solution from GoOSE (dashed), thanks to using expanders to explore the search space. The amplitude with the configuration of the autotuning (double dash-dotted) is the biggest, while the gains found by grid-free SafeOpt result in the smallest amplitude. The solution of grid SafeOpt (single dash-dotted) resulted in a smaller amplitude than the autotuning but bigger than the configuration found by grid-free SafeOpt.

We also note that the grid-free SafeOpt reaches the optimum error in iteration 60. This indicates the potential of using a stopping criterion based on convergence instead of number of iterations (Zagorowska et al., 2023). We also note that grid-free SafeOpt reached zero error at the same time as GoOSE, around 120 ms, whereas the autotuning needed 160 ms. This

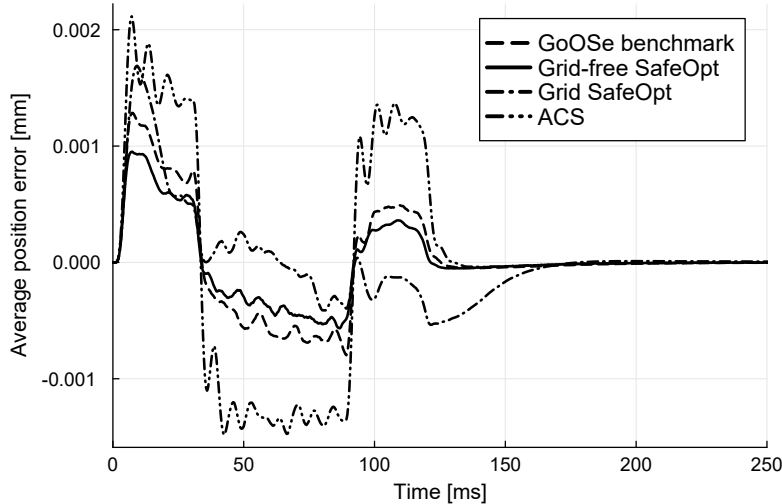


Figure 11: Position error comparison averaged over 10 runs, obtained for the optimal x^* from Table 5

result confirms the advantages of using an optimization-based tuning if high precision is required.

7. Conclusions and future work

Learning-based controller tuning allows adjusting the parameters that satisfy chosen performance criteria while satisfying safety constraints. In this work, we present a new approach to safe learning, formulating the SafeOpt algorithm as a series of local optimization problems, thus avoiding exhaustive search and improving its computational performance. We also develop a method for initializing the local optimization problems to ensure their feasibility, while preserving the properties of SafeOpt, thus enabling controller tuning without explicitly formulating the optimization problem as a function of the controller parameters.

The proposed grid-free SafeOpt algorithm has been first validated in a simulation of cascade controller tuning, showing the impact of initialization on local solvers and confirming improved computational performance. In particular, the initialization can be used to adjust the safe sets obtained during the optimization, thus improving the flexibility of the grid-free SafeOpt. We then demonstrate experimentally the performance of the algorithm for controller tuning in a precision motion system. A comparison with the default

autotuner shows the benefits of using optimization-based tuning to achieve the required sub-micrometer precision. The nearly seven-fold improvement in run-time compared to grid SafeOpt is achieved thanks to limiting the number of points during the search for the next iterate.

The experiments also show that the efficient SafeOpt implementation achieved 30% better tracking performance than a state-of-the-art benchmark algorithm, at the expense of a twice as long computational time. For this project, we used pattern search to solve the optimization problems in the grid-free SafeOpt. In the future, other optimization algorithms could potentially be used to further improve the run-time of the algorithm, which would enable its application in continuous optimization for use in time-varying systems.

Declaration of competing interest

The authors declare that they have no known competing financial interests or personal relationships that could have appeared to influence the work reported in this paper.

Acknowledgement

Research supported by NCCR Automation, a National Centre of Competence in Research, funded by the Swiss National Science Foundation (grant no. 180545), and by the European Research Council (ERC) under the H2020 Advanced Grant no. 787845 (OCAL). Marta Zagorowska also acknowledges funding from the Marie Curie Horizon Postdoctoral Fellowship project RELIC (grant no 101063948).

References

- Åström, K.J., Hägglund, T., 2006. *Advanced PID Control*. ISA-The Instrumentation, Systems, and Automation Society.
- Audet, C., Hare, W., 2017. *Derivative-free and blackbox optimization*. Springer Series in Operations Research and Financial Engineering, Springer Cham.
- Azizsoltani, H., Sadeghi, E., 2018. Adaptive sequential strategy for risk estimation of engineering systems using Gaussian process regression active learning. *Engineering Applications of Artificial Intelligence* 74, 146–165.

- Berkenkamp, F., Krause, A., Schoellig, A.P., 2021. Bayesian optimization with safety constraints: Safe and automatic parameter tuning in robotics. *Machine Learning* , 1–35.
- Berkenkamp, F., Schoellig, A.P., Krause, A., 2016. Safe controller optimization for quadrotors with Gaussian processes, in: 2016 IEEE International Conference on Robotics and Automation (ICRA), IEEE Press. p. 491–496.
- Bichon, B.J., McFarland, J.M., Mahadevan, S., 2011. Efficient surrogate models for reliability analysis of systems with multiple failure modes. *Reliability Engineering & System Safety* 96, 1386–1395.
- Bogunovic, I., Scarlett, J., Cevher, V., 2016. Time-varying Gaussian process bandit optimization, in: *Artificial Intelligence and Statistics*, PMLR. pp. 314–323.
- Duivenvoorden, R.R.P.R., Berkenkamp, F., Carion, N., Krause, A., Schoellig, A.P., 2017. Constrained Bayesian optimization with particle swarms for safe adaptive controller tuning. *IFAC-PapersOnLine* 50, 11800–11807.
- Fauriat, W., Gayton, N., 2014. AK-SYS: an adaptation of the AK-MCS method for system reliability. *Reliability Engineering & System Safety* 123, 137–144.
- Fiducioso, M., Curi, S., Schumacher, B., Gwerder, M., Krause, A., 2019. Safe contextual Bayesian optimization for sustainable room temperature PID control tuning, in: *Proceedings of the Twenty-Eighth International Joint Conference on Artificial Intelligence, IJCAI-19, International Joint Conferences on Artificial Intelligence Organization*. pp. 5850–5856.
- Fujimoto, Y., Sato, H., Nagahara, M., 2022. Controller tuning with Bayesian optimization and its acceleration: Concept and experimental validation. *Asian Journal of Control* 25, 2408–2414.
- Iman, R.L., Shortencarier, M.J., 1984. Fortran 77 program and user’s guide for the generation of Latin hypercube and random samples for use with computer models URL: <https://www.osti.gov/biblio/7091452>. accessed: 26 Sep 2023.

- Khosravi, M., Behrunani, V., Smith, R.S., Rupenyan, A., Lygeros, J., 2020. Cascade control: Data-driven tuning approach based on bayesian optimization. *IFAC-PapersOnLine* 53, 382–387. 21st IFAC World Congress.
- Khosravi, M., Behrunani, V.N., Myszkowski, P., Smith, R.S., Rupenyan, A., Lygeros, J., 2022. Performance-driven cascade controller tuning with Bayesian optimization. *IEEE Transactions on Industrial Electronics* 69, 1032–1042.
- Kim, Y., Allmendinger, R., López-Ibáñez, M., 2021. Safe learning and optimization techniques: Towards a survey of the state of the art, in: Heintz, F., Milano, M., O’Sullivan, B. (Eds.), *Trustworthy AI - Integrating Learning, Optimization and Reasoning*, Springer International Publishing, Cham. pp. 123–139.
- König, C., Ozols, M., Makarova, A., Balta, E.C., Krause, A., Rupenyan, A., 2023. Safe risk-averse Bayesian optimization for controller tuning. *IEEE Robotics and Automation Letters* , 1–8.
- König, C., Turchetta, M., Lygeros, J., Rupenyan, A., Krause, A., 2021. Safe and efficient model-free adaptive control via Bayesian optimization, in: 2021 IEEE International Conference on Robotics and Automation (ICRA), pp. 9782–9788.
- Lee, T., Tan, K., Huang, S., Dou, H., 2000. Intelligent control of precision linear actuators. *Engineering Applications of Artificial Intelligence* 13, 671–684.
- Mesbah, A., Wabersich, K.P., Schoellig, A.P., Zeilinger, M.N., Lucia, S., Badgwell, T.A., Paulson, J.A., 2022. Fusion of machine learning and MPC under uncertainty: What advances are on the horizon?, in: 2022 American Control Conference (ACC), IEEE. pp. 342–357.
- Rasmussen, C.E., Williams, C.K.I., 2006. *Gaussian Processes for Machine Learning*. Massachusetts Institute of Technology.
- Rothfuss, J., König, C., Rupenyan, A., Krause, A., 2022. Meta-learning priors for safe Bayesian optimization, in: *Conference on Robot Learning*, PMLR, Conference on Robot Learning, 14-18 December 2022, Auckland, New Zealand. pp. 237–265.

- Skogestad, S., 2023. Advanced control using decomposition and simple elements. *Annual Reviews in Control* 56, 100903.
- Srinivas, N., Krause, A., Kakade, S.M., Seeger, M.W., 2012. Information-theoretic regret bounds for Gaussian process optimization in the bandit setting. *IEEE Transactions on Information Theory* 58, 3250–3265.
- Sui, Y., Gotovos, A., Burdick, J., Krause, A., 2015a. Safe exploration for optimization with Gaussian processes, in: Bach, F., Blei, D. (Eds.), *Proceedings of the 32nd International Conference on Machine Learning*, PMLR, Lille, France. pp. 997–1005.
- Sui, Y., Gotovos, A., Burdick, J.W., Krause, A., 2015b. Safe exploration for optimization with Gaussian processes, in: *Proceedings of the 32nd International Conference on Machine Learning*, Lille, France. pp. 997–1005.
- Sukhija, B., Turchetta, M., Lindner, D., Krause, A., Trimpe, S., Baumann, D., 2023. GoSafeOpt: Scalable safe exploration for global optimization of dynamical systems. *Artificial Intelligence* 320, 103922.
- Swersky, K., Snoek, J., Adams, R.P., 2013. Multi-task Bayesian optimization, in: Burges, C., Bottou, L., Welling, M., Ghahramani, Z., Weinberger, K. (Eds.), *Advances in Neural Information Processing Systems (NIPS 2013)*, Curran Associates, Inc.. pp. 2004–2012.
- Xu, Z., Saleh, J.H., 2021. Machine learning for reliability engineering and safety applications: Review of current status and future opportunities. *Reliability Engineering & System Safety* 211, 107530.
- Zagorowska, M., Balta, E.C., Behrunani, V., Rupenyan, A., Lygeros, J., 2023. Efficient sample selection for safe learning, in: *IFAC World Congress 2023*. Online: 20.500.11850/615589.